

Open Nanoporous Morphologies from Polymeric Blends by Carbon Dioxide Foaming

B. Krause, K. Diekmann, N. F. A. van der Vegt,* and M. Wessling

Membrane Technology Group, University of Twente, P.O. Box 217,
7500 AE Enschede, The Netherlands

Received September 24, 2001

ABSTRACT: We report the formation of open nanoporous polymer films composed of homogeneous polysulfone/polyimide blends. Porosity is introduced by expansion of carbon dioxide-saturated films at elevated temperatures. To interpret details of the porous morphologies in terms of the experimental conditions during expansion, the glass transition temperature and carbon dioxide solubility of the dense film were examined at various blend compositions. We find that above a critical threshold of the carbon dioxide concentration the porous structure obtained changes from microcellular into open nanoporous. This critical carbon dioxide concentration is independent of the blend composition. Remarkably, it resembles the value previously reported on different polymers.

1. Introduction

Nanoporous polymers with a well-defined open pore structure and tunable mass transport characteristics are of major importance in drug delivery devices^{1,2} and porous membrane materials for liquid separations. Today, these materials are mainly prepared by phase inversion of polymer solutions.³ The demixing process, which stops at the vitrification point of the polymer-rich phase, can be initiated either by a temperature quench or by diffusive solvent–nonsolvent exchange (immersion precipitation) of binary, ternary, or multi-component mixtures. A serious drawback of these techniques is the presence of solvents during the preparation procedure. In addition to not being environmentally benign, the solvent contaminates the porous material and often needs to be removed in excessive posttreatment processes. Partially, these contaminants are removed by intense washing procedures. However, for medical and pharmaceutical applications, totally solvent-free membrane materials are required.

Only a limited number of techniques allow the preparation of solvent-free membrane materials: (i) controlled stretching of homogeneous semicrystalline polymers such as poly(tetrafluoroethylene)⁴ and polypropylene⁵ and (ii) the track-etching process⁶ of polycarbonate, poly(ethylene terephthalate), and polyimide. However, both techniques do not allow the preparation of nanoporous materials. An alternative way to introduce nanoporosity is based on the thermal treatment of high- T_g polymers blended with thermally unstable components (polymers or organic components).^{7,8} If the content of the thermally unstable component exceeds the percolation threshold, bicontinuous morphologies are expected. This technique has proven to be successful in the production of low- k polymers.⁹ Drawbacks of this technique are that on one hand only a limited number of polymers are stable during the thermal decomposition of the labile component. Also, the added porogen might contaminate the parent polymer matrix if not fully degradable.

Our approach to prepare additive-free membranes consists of the foaming of polymers with carbon dioxide

as physical-blowing agent, which vanishes from the polymer matrix during the foaming procedure without leaving any residue behind. Foamed polymer structures are obtained by expanding the gas-saturated sample against atmospheric pressure at temperatures above the glass transition temperature. Such foaming procedures for glassy polymers have been the subject of investigation for a long time;¹⁰ however, only closed cellular structures with characteristic cell dimensions above 10 μm were obtained.

Recently, we have reported “foam diagrams” for high- T_g polymers clarifying foam characteristics (cell densities, mass densities) in terms of the CO_2 saturation conditions and the foaming temperature.¹¹ In particular, we identified a critical carbon dioxide concentration, c_{crit} , required to obtain a transition from closed cellular structures to open nanoporous morphologies. Employing poly(ether sulfone) and poly(ether imide) films, it was shown that at least 48 cm^3 of CO_2 (STP)/ cm^3 (polymer) is required to obtain open nanoporous structures. This high carbon dioxide saturation level restricts the number of polymers being suitable for this technique, because very few polymers possess a sorption capacity for carbon dioxide above c_{crit} under nonsupercritical conditions.¹²

In this work, we study the foaming behavior of polymer films composed of polyimide (Matrimid), polysulfone, and their blends using the discontinuous solid-state foaming technique^{13,14} with carbon dioxide as a physical blowing agent. We will report blending of polymers as a means to systematically adjust the sorption capacity of the blends, which enable us to control the morphology of the final porous structures. Open nanoporous morphologies can be prepared if the carbon dioxide concentration of the saturated film prior to the foaming step is above $50 \pm 3 \text{ cm}^3$ (STP)/ cm^3 (polymer). This critical concentration does not depend on the blend composition. Concentrations below this value lead to closed microcellular structures.

In section 2 we describe the experimental details. In section 3.1 we present the blend characteristics, viz., carbon dioxide sorption behavior up to 50 bar at 25 °C and glass transition temperature data of the blends and the parent polymers. The preparation of micro- and

* Corresponding author: e-mail n.f.a.vandervegt@ct.utwente.nl.

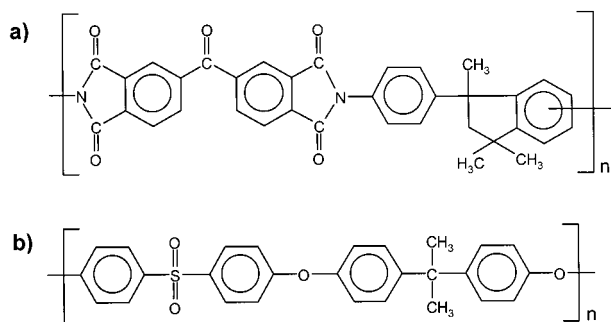


Figure 1. Chemical structures of the (a) polyimide (Matrimid) and (b) bisphenol A polysulfone monomer units.

nanocellular blends is discussed in section 3.2. On the basis of helium permeation measurements, the critical CO₂ concentration to produce open nanoporous films will be located.

2. Experimental Section

2.1. Materials. Two commercially available polymers, bisphenol A polysulfone (PSU), type Udel P-3500, received from Amoco Chemicals, Belgium, and a polyimide (PI), type Matrimid 5218, received from Ciba Specialty Chemicals, Switzerland, are used in this work. The chemical structure of both polymers is shown in Figure 1. Dichloromethane, glycerol, and hexane were purchased from Merck (analytical grade) and used as received. Carbon dioxide was purchased from Praxair having purity a larger than 99.99%.

2.2. Film Preparation. The polymers are used as received without further purification for film formation. Solutions of PSU, PI, and their blends are prepared by dissolving 20 wt % polymer in dichloromethane. The mass compositions of the prepared blends are 1/9, 2/8, 4/6, 5/5, 6/4, and 8/2. Thin films of around 100 μ m thickness are prepared by solution-casting on a glass plate. The casted films are dried in a nitrogen atmosphere at room temperature for 24 h. The homogeneous dense PSU, PI, and blend films thus obtained are removed from the glass plate with the help of a small amount of water and are dried for several days under nitrogen atmosphere at 195, 250, and 200 $^{\circ}$ C, respectively. The dry films (thickness \sim 75 μ m) are analyzed using elemental analysis (CI) to determine remaining dichloromethane traces. The remaining solvent concentrations were all found smaller than 0.03 wt %. The presence of residual solvent traces (>0.05 wt %) in the polymer film can cause open-cell formation.¹⁵

2.3. Polymer Film Characterization. The polymer films are characterized to determine their glass transition temperature (T_g), mass density, and carbon dioxide sorption characteristics. A Perkin-Elmer differential scanning calorimeter DSC7 is used to determine the glass transition temperature of the films used. The T_g is obtained from the first run, using a heating rate of 20 K/min. The mass densities of the foamed polymer samples are analyzed by using the flotation weight loss method (ASTM D-792) with hexane as liquid. Hexane uptake in the foamed sample could not be observed during the measurement, which process would overestimate the true density.

The equilibrium sorption of carbon dioxide into the polymer films is measured using a dual volume setup similar to the one described by Koros et al.^{16,17} The equipment used and the experimental procedure of the sorption measurements are described elsewhere.¹⁸ Sorption isotherms for the pressure range up to 50 bar at 25 $^{\circ}$ C are determined for all films.

2.4. Foam Formation Technique. Dense polymer films are cut into 4 cm \times 4 cm pieces and placed in a pressure vessel connected to a carbon dioxide cylinder. The samples are next saturated with carbon dioxide at room temperature (25 $^{\circ}$ C) and elevated pressure (10–50 bar). Subsequently, the carbon dioxide pressure is quickly released from the pressure vessel (within 1 s). After removing the gas-saturated polymer film from the pressure vessel, the sample is immersed in a glycerol

bath maintained at the desired temperature (foaming temperature) for 30 s (foaming time). If the foaming temperature surpasses the glass transition temperature of the saturated film, the polymer expands and a porous film remains. The porous samples are next quenched in an ethanol/water (1 + 1) mixture and washed in ethanol for a least 1 h. The washing procedure in ethanol is performed to remove adhesive glycerol traces and does not have any effect on the morphology of the foam. Subsequently, the samples are dried under vacuum (Heraeus VT 6060M in combination with an Edwards RV3 rotary vane pump) at 30 $^{\circ}$ C for 24 h to remove traces of ethanol and water. The porous films always exhibit dense skin parts due to the CO₂ loss from the surface regions prior to the foaming step. A more detailed description of the process and the influence of the experimental conditions is given elsewhere.¹⁴

2.5. Foam Characterization. The foamed polymer films are characterized with regard to their mass densities and open porosity.

The mass densities of the foamed polymer samples are analyzed by using the flotation weight loss method (ASTM D-792) with hexane as liquid. Hexane uptake in the foamed sample is not observed during the measurement, due to the dense skin parts covering the porous substructure. The obtained mass densities are average values of the entire polymer sample, i.e., the foamed core part including the integral dense skin. The microcellular morphologies of the foamed samples are investigated using a JEOL JSM 5600 LV and a JEOL JSM T220A scanning electron microscope (SEM). The samples are freeze-fractured in liquid nitrogen and sputter-coated (Balzers/Union 040) with gold at an argon pressure of 0.1 Torr for 2 min at a current of 13 mA. To characterize the onset to open porosity, helium permeation measurements are performed using self-made gas flux modules. A detailed description of the module preparation and the measurement conditions is given elsewhere.¹⁵ The normalized helium flux (P/L) through the sample is expressed in m³/(m² h bar). The active measurement area is calculated from the measured width of the sample and the average thickness, which is corrected for the dense unfoamed skin on the basis of SEM investigations of the cross section of the foamed sample. The thickness of the integral skin is determined using the method described by Kumar and Weller.¹⁹

3. Results and Discussion

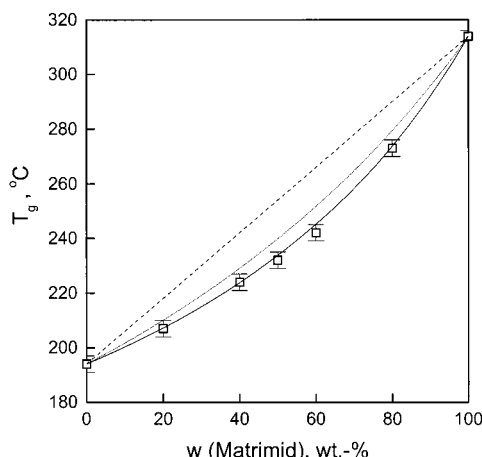
3.1. Characterization of the Polymers/Blends. The glass transition temperature and the gas sorption behavior of the polymers and polymer blends investigated here are of major importance because both characteristics crucially influence the polymer expansion process and the resulting porous morphology. The glass transition temperature of the polymer/polymer blend determines the lower foaming temperature boundary, T_{lower} .¹⁴ The amount of dissolved carbon dioxide controls (i) the lower boundary foaming temperature, T_{lower} , and (ii) the foam morphology, i.e., the cell size and the cell density.

The glass transition temperature of Matrimid/polysulfone blends was already investigated earlier,^{20,21} and it was found that solution-casted films form homogeneous blends. However, these blends phase separate after annealing them at a temperature above the T_g of Matrimid. We report in Table 1 the glass transition temperature of Matrimid, polysulfone, and their blends obtained from the first run (homogeneous blends). The glass transition data are presented graphically in Figure 2. Three different equations are applied to model the experimental data: (a) the linear mixing rule, (b) the Fox equation ($1/T_g = (w_1/T_{g1}) + (w_2/T_{g2})$) which assumes an "ideal" volume additivity, and (c) a modified Gordon–Taylor equation ($(T_g - T_{g1})/(T_{g2} - T_{g1}) = (1 + K_1)w_{2c} -$

Table 1. Mass Density and Glass Transition Temperature for PSU, Matrimid (PI), and Their Blend Films at 25 °C^a

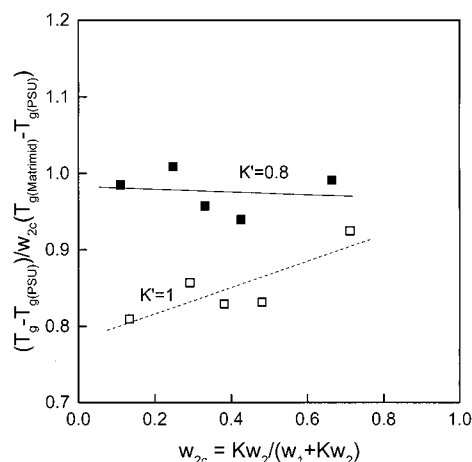
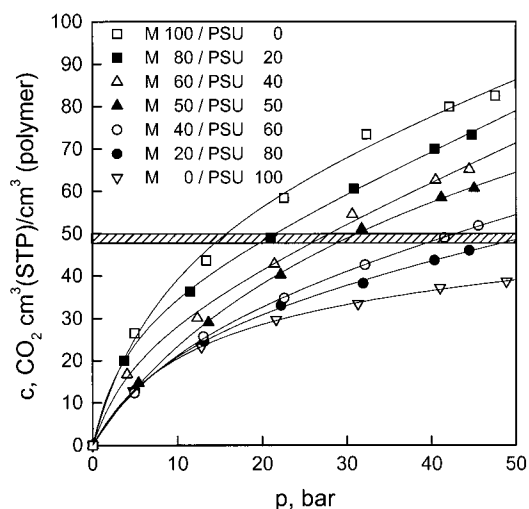
	PSU	2/8	4/6	5/5	6/4	8/2	PI
T_g , °C	194	207	224	232	242	273	314
mass density, g/cm ³	1.24	1.24	1.24	1.24	1.24	1.24	1.23

^a The composition of the blends is expressed by their mass ratio of PSU and PI: the first value expresses the amount PSU, and the second value expresses the amount PI. The glass transition temperature values given are obtained from the first run.

**Figure 2.** Composition dependence of the glass transition temperature of blends of Matrimid and polysulfone. The data are fitted with (a) the linear mixing rule (dashed line), (b) the Fox equation (dotted line), and (c) the modified Gordon–Taylor equation with $K = K'T_{g1}/T_{g2}$ ($K' = 0.8$).

$(K_1 + K_2)w_{2c}^2 + K_2 w_{2c}^3$ proposed by Schneider,^{22,23} where $w_{2c} = Kw_2/(w_1 + Kw_2)$ represents the corrected weight fraction of component 2 (with the higher glass transition temperature T_{g2}) and K is defined as the ratio of the differences of coefficients of expansion, $\Delta\alpha$, at T_g of the glassy and rubbery states. K_1 and K_2 are related to the differences between the parts of binary interaction energies of hetero- and homocontacts to be overcome at T_g .²³ For blend components with identical interactions between chain segments, both $K_1 = 0$ and $K_2 = 0$ (ideal volume additivity) and $(T_g - T_{g1})/(T_{g2} - T_{g1})w_{2c}$ will result in a horizontal line about unity when represented versus w_{2c} . The linear mixing rule (a) and the Fox equation (b) do not fit our experimental data. Applying the modified Gordon–Taylor equation (c) results in a negative deviation from volume additivity (Figure 3). The observed slight negative deviation supports the observed weak intermolecular interaction for the Matrimid/polysulfone blends²⁰ and similar Matrimid/poly(ether sulfone) blends.²⁴ However, this negative deviation of the T_g -composition data from the volume additivity rule characterized by²³ $K = K'T_{g1}/T_{g2}$ ($K' = 1$) can be almost compensated by changing the K' coefficient to 0.8. Applying the modified Gordon–Taylor equation with $K' = 0.8$ results in a perfect fit of our experimental T_g data, shown in Figure 2.

The carbon dioxide sorption behavior of the parent materials and their blends are investigated up to a maximum pressure of 50 bar at 25 °C. The sorption isotherms shown in Figure 4 are concave to the pressure axis, common for gas sorption in glassy polymeric solvents. The sorption capacity increases with increasing Matrimid content (the component with the highest T_g), and all blend materials show sorption behavior which lies in between the parent materials. The dashed

**Figure 3.** Representation of the T_g -composition behavior of blends of Matrimid and polysulfone (PSU) according to Schneider²³ using different values of the K parameter, $K = K'T_{g1}/T_{g2}$ ($K' = 1.0$) ($K' = 0.8$).**Figure 4.** Sorption isotherms of CO₂ in Matrimid (M), polysulfone (PSU), and their blends at 25 °C. (Value behind M and PSU correspond to the weight percentage of the component in the blend; symbols are experimental values, lines represent the dual mode sorption model fit;²⁵ the dashed region between 48 and 50 cm³ (STP)/cm³ (polymer) corresponds to the threshold concentration required to form open foam morphologies.¹¹)

region between 48 and 50 cm³ (STP)/cm³ (polymer) corresponds to the critical concentration required to form open foam morphologies¹¹ for poly(ether imide) and poly(ether sulfone). If our concept of a critical concentration applies to the materials investigated here as well, one expects to observe a transition in foam morphology if the dissolved amount of carbon dioxide raises above the dashed range. We discuss this in section 3.2.

The carbon dioxide sorption behavior of the blends at an equilibrium pressure of 50 bar follows an ideal mixing rule as shown in Figure 5. In fact, one expects this behavior for homogeneous (compatible) blends assuming ideal volume additivity. A similar behavior is observed for the sorption of carbon dioxide and methane in miscible amorphous polystyrene (PS)/poly(phenylene oxide) (PPO) blends^{26,27} in a pressure range up to 22 bar at 35 °C. The measured T_g data of PPO/PS blends²³ show a negative deviation from the ideal T_g behavior, comparable to our observation.

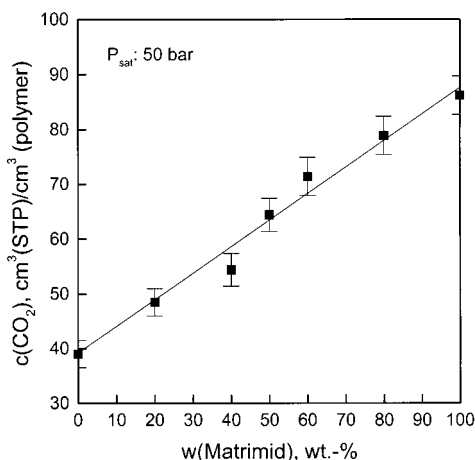


Figure 5. Carbon dioxide sorption capacity dependent on the blend composition (Matrimid/PSU) at 50 bar (P_{sat}) and 25 °C. The error bars indicate the calculated error for the sorbed amount of carbon dioxide based on the method applied to determine the sorption isotherms.

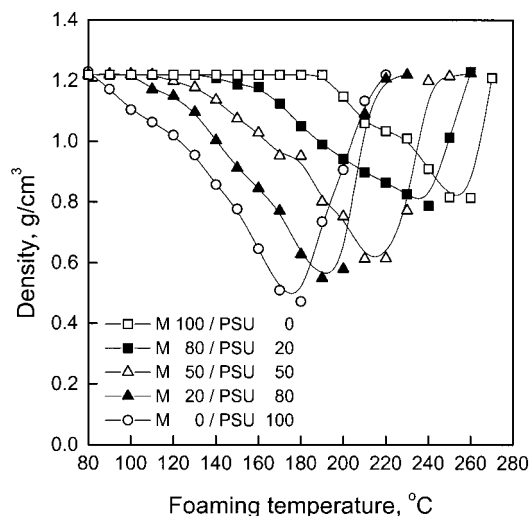


Figure 6. Mass density of Matrimid (M), polysulfone (PSU), and their blends dependent on foaming temperature for samples saturated with 50 bar of carbon dioxide at 25 °C. (Value behind M and PSU correspond to the weight percentage of the component in the blend.)

3.2. Foaming Behavior of Matrimid, Polysulfone, and Their Blends. Expansion of dense carbon dioxide saturated films occurs in a “foaming region” bound by two temperatures: (1) a lower bound temperature, T_{lower} , which corresponds to the glass transition temperature of the polymer/gas mixture and depends strongly on the CO_2 content of the saturated film, and (2) an upper bound temperature, T_{upper} , where cells are destabilized due to diffusion of carbon dioxide out of the material (T_{upper} is generally close to the T_g of the carbon dioxide-free film).^{11,14}

To investigate the foaming behavior of the parent materials and their blends, foaming experiments are performed after saturating all samples at a pressure of 50 bar at 25 °C. Because of the different sorption capacities (Figure 4), the carbon dioxide concentration varies between 39 and 86 cm^3 (STP)/ cm^3 (polymer) for PSU and Matrimid, respectively. The mass densities of the porous films of PSU, Matrimid, and three blends of these two polymers as a function of the foaming temperature are shown in Figure 6. Foaming starts at the T_g of the saturated film where the mass density first

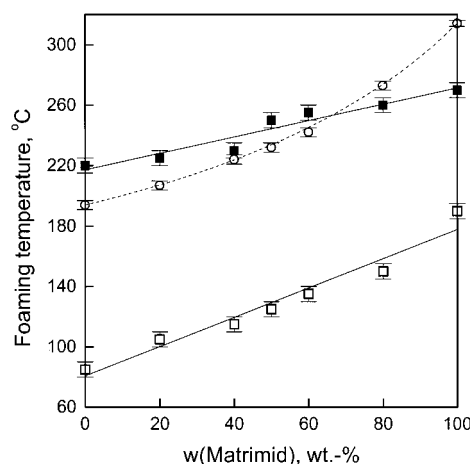


Figure 7. T_{lower} (□) and T_{upper} (■) as a function of the blend composition and the foaming temperature. The samples used for determining T_{upper} and T_{lower} were saturated with 50 bar of carbon dioxide at 25 °C. For comparison, the glass transition temperature of the pure (carbon dioxide free) blends (○) are shown. The straight lines (T_{lower} , T_{upper}) represent a least-squares fit of the experimental data. The dashed line (T_g of the carbon dioxide-free polymer blend) represents the modified Gordon–Taylor equation with $K = K' T_{g1}/T_{g2}$ ($K' = 0.8$) (see Figure 2).

drops below that of the dense sample. This point shifts to higher temperatures with increasing Matrimid content in the blend as expected on the basis of the composition-dependent T_g of the dry (CO_2 -free) blend composition (Figure 2). Accompanied by the increase of T_{lower} is a simultaneous increase of the upper temperature limit, T_{upper} . At T_{upper} the mass density of the foamed sample equals the density of the dense film. The glass transition temperature of the carbon dioxide-free blends and the dependence of T_{upper} and T_{lower} on the blend composition and the foaming temperature are presented in Figure 7. For polysulfone T_{upper} lies at approximately 220 °C, which is 26 °C above the T_g of pure PSU. Matrimid, on the other hand, shows an upper temperature limit at approximately 270 °C, which is 44 °C below its T_g . The upper temperature above which porosity can no longer be introduced is strongly determined by the diffusion rate in which CO_2 leaves the sample.¹⁴

The temperatures at which a minimum mass density is observed (Figure 6) increases with increasing Matrimid content. We will refer to this temperature as T_{max} (at this temperature a maximum in the cell density occurs). This shift expresses the general tendency that the expansion reaches a maximum close to the T_g of the carbon dioxide-free material. Above T_{max} , a major part of the dissolved carbon dioxide does not partake in expansion but is lost from the sample by diffusion. We note here that in our experiments all samples were saturated at a constant pressure of 50 bar. This means that the CO_2 concentrations varied for each blend composition. In general, T_{max} shifts slightly to higher temperatures if the CO_2 concentration (the extent of plasticization) decreases. For example, a variation in saturation pressure from 50 to 20 bar (a decrease of approximately 40 cm^3 (STP)/ cm^3 (polymer)) leads to an increase of T_{max} by 10 °C for Matrimid samples. An increase of approximately 5 °C of T_{max} could be observed for a blend containing 40 wt % Matrimid and 60 wt % PSU by lowering the CO_2 saturation pressure from 50 to 30 bar (a decrease of approximately 20 cm^3 (STP)/

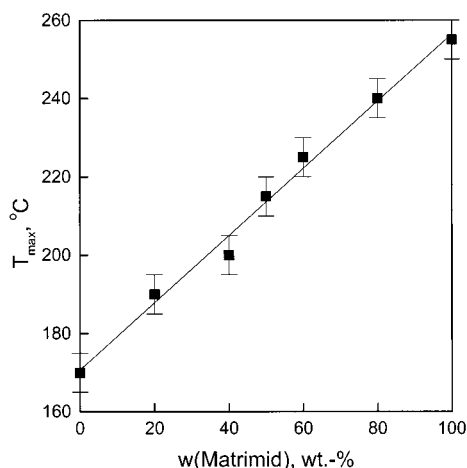


Figure 8. Foaming temperatures (T_{\max}) leading to maximum porosity presented vs the Matrimid/PSU blend compositions. The error bars are obtained from two repeated series of foaming experiments.

cm^3 (polymer)). T_{\max} is presented as a function of the blend composition in Figure 8. A linear relationship can be observed, despite large differences between the carbon dioxide concentration of the samples prior to foaming. This ideal behavior actually allows to predict the temperature T_{\max} at which optimized porosities of homogeneous blends are achieved based on T_{\max} of the two parent materials only.

It has to be mentioned here that foam samples with different blend composition and prepared at different foaming temperatures do not show any indication of phase separation. This we confirmed on the basis of DSC experiments and is consistent with the observations in earlier work¹⁴ as the foaming temperature never raises above the T_g of the pure Matrimid. A short foaming time (30 s) in which the temperature is raised above the T_g of the CO_2 plasticized film apparently is insufficient to induce phase separation.

The cellular morphologies strongly depend on the dissolved amount of carbon dioxide available during expansion of the sample. It has been shown earlier that poly(ether imide) and poly(ether sulfone) exhibit a transition from a closed-cellular structure to an open nanoporous structure if the carbon dioxide concentration is raised above a critical value, c_{crit} , of approximately 48 cm^3 (STP)/ cm^3 (polymer).¹¹ If this critical carbon dioxide concentration applies in a more general sense to a wider variety of polymers, we should observe a transition to open nanoporous films at the same CO_2 concentration for all polyimide/polysulfone blend compositions investigated here.

The cellular morphologies of the two pure blend components are presented in Figures 9A,B. Both samples were saturated at a CO_2 pressure of 50 bar and foamed at their T_{\max} . At 50 bar, the CO_2 concentration in PSU lies below c_{crit} , whereas that in Matrimid lies well above c_{crit} (see Figure 4). The polysulfone sample shows a closed-cell structure as already presented earlier.¹⁴ In Figure 9A, we observe closed cells with characteristic cell diameters of approximately $1 \mu\text{m}$. The polyimide foam in Figure 9B displays an open nanoporous structure. The characteristic cell dimensions are on the order of 20–50 nm. The exact location of c_{crit} for Matrimid and the blends with polysulfone will be shown to coincide with the critical CO_2 content illustrated in Figure 4 on

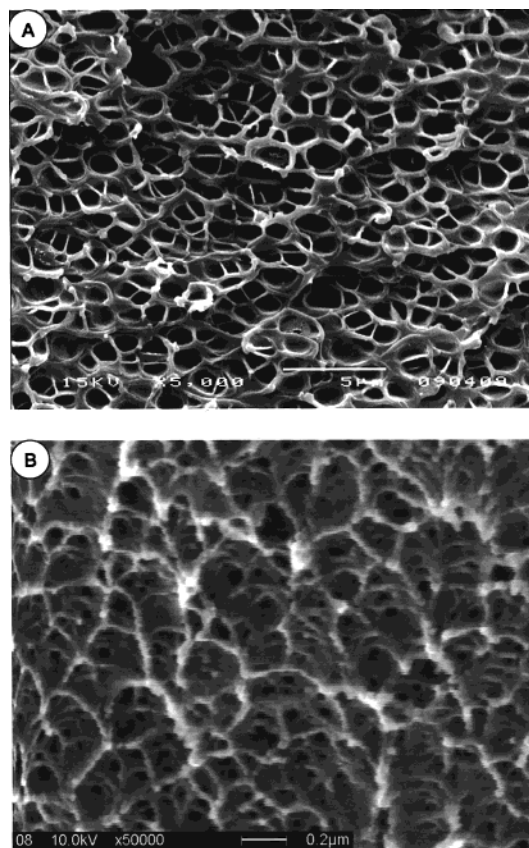


Figure 9. SEM micrographs of PSU (A) and Matrimid (B) films, which were saturated at 50 bar of carbon dioxide and foamed at 170 and 260 °C, respectively. Magnification: (A) 5000, the white horizontal bar indicates $5 \mu\text{m}$; (B) 50 000, the white horizontal bar indicates 200 nm.

the basis of helium permeation tests which we will discuss later.

To study the foam morphologies of films with different blend compositions, all samples were saturated at 50 bar of carbon dioxide and 25 °C. SEM micrographs of two different blends are shown in Figure 10. Sample A contained 50 wt % Matrimid whereas the Matrimid content in sample B was 80 wt %. The foaming temperatures were 210 and 240 °C, respectively. Both samples clearly show a nanoporous morphology with opening well below 500 nm. The size of these openings seems to be dependent on the blend composition.

To provide irrefutable proof of having obtained open porous structures, gas permeation measurements are performed. Because of the presence of the dense skins, the gas flux could not be measured perpendicular to the film but had to be measured in the lateral direction through the porous morphology. Detailed information about the measurement setup is given elsewhere.¹⁵ The helium fluxes were measured for all foamed PSU, Matrimid, and blend morphologies. The pressure normalized fluxes (P/L in $\text{m}^3/(\text{m}^2 \text{ h bar})$) are presented in Figure 11 for foam samples with different blend compositions prepared at a saturation pressure of 50 bar and different foaming temperatures. For all blend compositions (40 and 60 wt % Matrimid not shown) and for pure Matrimid a gas flux was detected. The value of the helium permeance as well as the foaming temperature window where open structures are formed increases with increasing polyimide content. The blend composition of 20 wt % Matrimid reaches a CO_2 concentration of 50 cm^3 (STP)/ cm^3 (polymer) at 50 bar

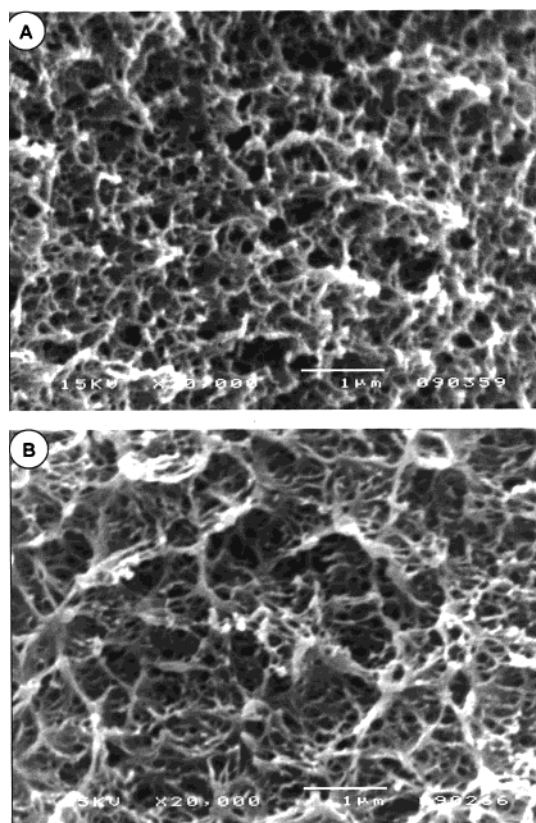


Figure 10. SEM micrographs of blends containing (A) 50 wt % Matrimid and 50 wt % PSU and (B) 80 wt % Matrimid and 20 wt % PSU, which were saturated at 50 bar of carbon dioxide and foamed at 210 and 240 °C, respectively. Magnification: 20 000, the white horizontal bar indicates 1 μm .

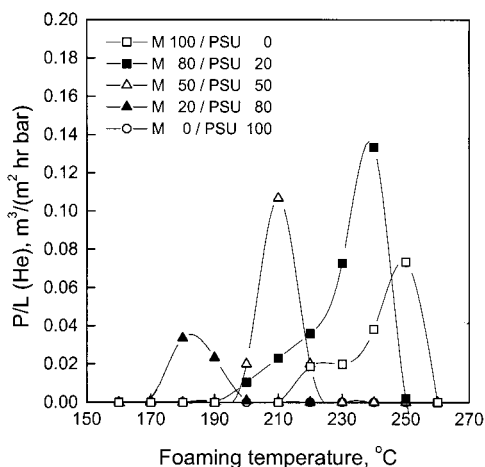


Figure 11. Normalized helium flux (P/L in $\text{m}^3 \text{m}^{-2} \text{bar}^{-1} \text{h}^{-1}$) through the cross section of Matrimid (M), polysulfone (PSU), and their blends vs the foaming temperature. Films were saturated at 50 bar of carbon dioxide (25 °C) prior to foaming. The values behind M and PSU correspond to the weight percentage of the component in the blend.

CO_2 pressure (Figure 4), which is just enough to obtain an open structure permeable to helium. The film composed of pure polysulfone reaches a concentration of $39 \text{ cm}^3 (\text{STP})/\text{cm}^3$ (polymer) at 50 bar (Figure 4), which is below c_{crit} . Hence, no helium fluxes could be detected.

To identify the exact carbon dioxide concentration required to form open morphologies, two different blend compositions and pure Matrimid were saturated at variable carbon dioxide pressure and foamed at tem-

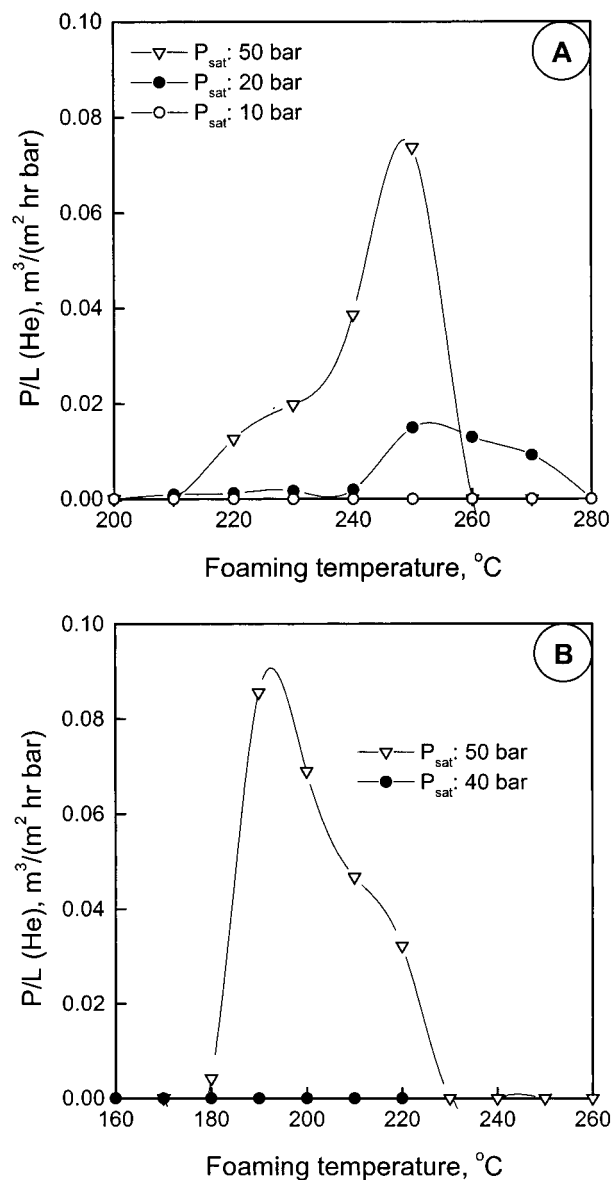


Figure 12. Normalized helium flux (P/L in $\text{m}^3 \text{m}^{-2} \text{bar}^{-1} \text{h}^{-1}$) through the cross section of Matrimid (A) and a blend containing 40 wt % Matrimid and 60 wt % polysulfone (B) vs the foaming temperature. Films were saturated at the carbon dioxide pressures (25 °C) indicated in the figure.

peratures between T_{lower} and T_{upper} . Helium permeation tests were performed to verify whether open structures were obtained. The permeation results of two materials are presented in Figure 12. Porous Matrimid (Figure 12A) shows a helium flux for samples that were saturated at 50 and 20 bar of CO_2 ; however, samples saturated at 10 bar do not show any helium permeance (no degree of openness). The CO_2 concentration in the blend (40 wt % Matrimid, 60 wt % PSU) (Figure 12B) seems to surpass c_{crit} somewhere in between the CO_2 saturation pressure of 40–50 bar. From these permeation experiments the critical carbon dioxide concentration required to form open morphologies was calculated. For Matrimid, the blend material containing 80 wt % Matrimid (permeation data not shown), and another blend containing 40 wt % Matrimid c_{crit} amounts to 48 ± 3 , 53 ± 3 , and 51 ± 3 ($\text{STP})/\text{cm}^3$ (polymer), respectively. These data are in excellent agreement with the value of c_{crit} reported for poly(ether imide) and poly(ether sulfone).¹¹

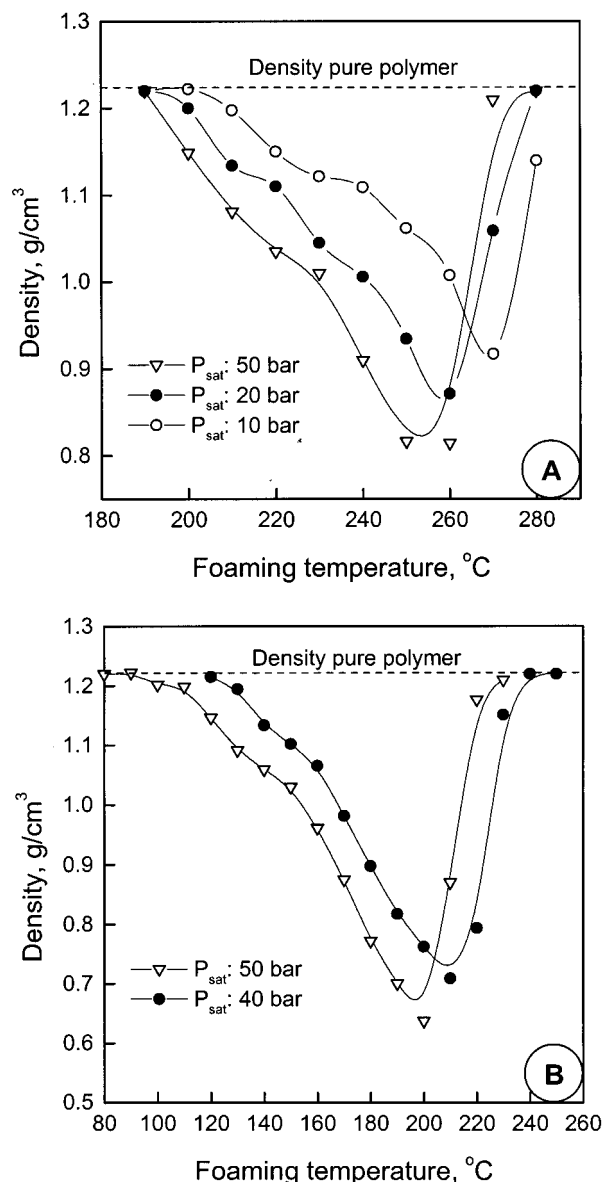


Figure 13. Mass density of Matrimid (A) and a blend containing 40 wt % Matrimid and 60 wt % polysulfone (B) vs the foaming temperature. Films were saturated at the carbon dioxide pressures (25 °C) indicated in the figure.

To show that the sudden onset and disappearance in the helium permeance is a result of a clear transition in morphology and not an effect of a strongly reduced porosity or any other effect based on reducing the carbon dioxide concentration present in the polymer prior to the foaming step, mass density measurements and morphology investigations are carried out. The mass densities for Matrimid and one blend composed of 40 wt % Matrimid and 60 wt % PSU are shown for different saturation pressures in Figure 13A,B as a function of the foaming temperature. In Figure 13A, the samples saturated at 50 and 20 bar are open; the one saturated at 10 bar has closed cells. In Figure 13B, the sample saturated at 50 bar is open and the other is closed. Both samples show only a slight decrease in porosity with decreasing carbon dioxide saturation pressure. This is supported by SEM micrographs (Figure 14) of the blend containing 40 wt % Matrimid and 60 wt % PSU saturated at 50 bar (A) and 40 bar (B) carbon dioxide pressure and foamed at 200 °C. In Figure 14A an open-cellular structure is observed, whereas Figure 14B

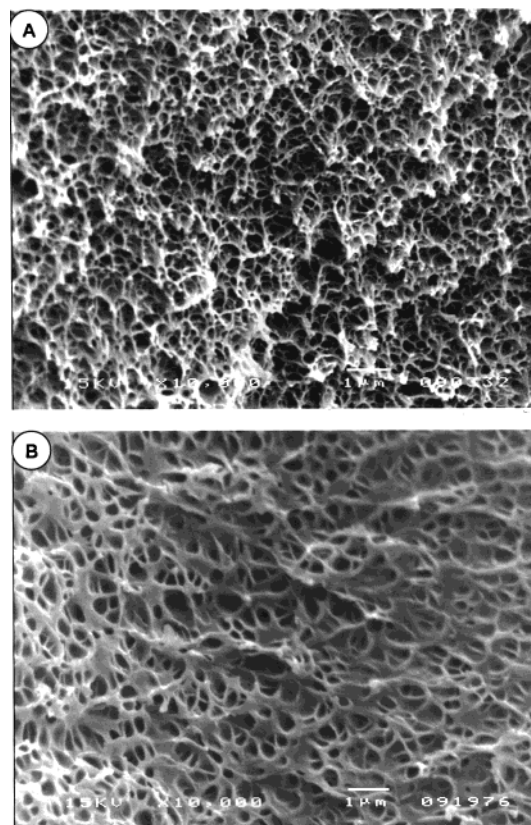


Figure 14. SEM micrographs of blends containing 40 wt % Matrimid and 60 wt % PSU saturated at 50 (A) and 40 bar (B) carbon dioxide pressure at 25 °C prior to foaming. Both samples were foamed at 200 °C. Magnification: 20 000, the white horizontal bar indicates 1 μm.

shows a closed-cellular structure. Both the SEM micrographs (Figure 14) and the mass densities (Figure 13) are representative for all materials used. We conclude that only the amount of carbon dioxide available in the film is responsible for the transition from a closed-cell morphology to an open nanoporous morphology.

4. Conclusions

Microcellular and open nanoporous polymer films were prepared by expansion of carbon dioxide-saturated precursor films composed of polysulfone/polyimide blends. For all polysulfone/polyimide compositions homogeneous dense films were prepared whose glass transition temperature could be well described using a modified Gordon–Taylor equation. The carbon dioxide sorption capacity of the blends follows an ideal mixing rule. During the expansion of the carbon dioxide-saturated films, two parameters are of major importance: (1) the temperature during expansion and (2) the carbon dioxide concentration in the saturated film. The temperature should be well above the glass transition temperature of the saturated film but below the glass transition temperature of the unsaturated (unplasticized) blend. The carbon dioxide concentration determines the ultimate porous structure to a large extent. At low concentrations (closed) microcellular structures are found, and at high concentrations we find (open) nanoporous structures. The transition from microcellular to nanoporous occurs in a narrow window of the carbon dioxide saturation level (we define this as the critical carbon dioxide concentration). This concentration amounts to $50 \pm 3 \text{ cm}^3 \text{ (STP)/cm}^3 \text{ (polymer)}$ and agrees with the

value we reported earlier for poly(ether sulfone) and poly(ether imide).

References and Notes

- (1) Brannon-Peppas, L. *Med. Plast. Biomater. Mag.* **1997**, Nov, 34.
- (2) Baker, R. *Controlled Release of Biologically Active Agents*; Wiley: New York, 1987.
- (3) Mulder, M. *Basic Principles of Membrane Technology*; Kluwer Academic Publisher: Dordrecht, 1996.
- (4) Gore, R. W. US Patent 3,953,566, 1973.
- (5) Druin, M. L.; Loft, J. T.; Plovan, S. G. US Patent 3,801,404, 1972.
- (6) Zeman, L. J.; Zydney, A. L. *Microfiltration and Ultrafiltration: Principles and Application*; Marcel Dekker: New York, 1996.
- (7) Takeichi, T.; Zuo, M.; Ito, A. *High Perform. Polym.* **1999**, *11*, 1–14.
- (8) Xu, Y.; Tsai, Y.; Tu, K. N.; Zhao, B.; Liu, Q.-Z.; Brongo, M.; Sheng, G. T. T.; Tung, C. H. *Appl. Phys. Lett.* **1999**, *75*, 853–855.
- (9) Miller, R. D. *Science* **1999**, *286*, 421–423.
- (10) Kazarian, S. G. *Polym. Sci., Ser. C* **2000**, *42*, 78–101.
- (11) Krause, B.; Sijbesma, H. J. P.; Mönüklü, P.; Van der Vegt, N. F. A.; Wessling, M. *Macromolecules* **2001**, *34*, 8792–8801.
- (12) Paterson, R.; Yampolskii, Y. P. *J. Phys. Chem. Ref. Data* **1999**, *28*, 1255–1451.
- (13) Kumar, V.; Weller, J. E. *Int. Polym. Process.* **1993**, *8*, 73–80.
- (14) Krause, B.; Mettinkhof, R.; Van der Vegt, N. F. A.; Wessling, M. *Macromolecules* **2001**, *34*, 874–884.
- (15) Krause, B.; Boerrigter, M. E.; Van der Vegt, N. F. A.; Strathmann, H.; Wessling, M. *J. Membr. Sci.* **2001**, *187*, 181–192.
- (16) Koros, W. J.; Paul, D. R.; Rocha, A. A. *J. Polym. Sci., Polym. Phys. Ed.* **1976**, *14*, 687–702.
- (17) Koros, W. J.; Paul, D. R. *J. Polym. Sci., Polym. Phys. Ed.* **1976**, *14*, 1903–1907.
- (18) Bos, A. High Pressure CO₂/CH₄ Separation with Glassy Polymer Membranes. Ph.D. Thesis, University of Twente, 1996.
- (19) Kumar, V.; Weller, J. E. *Polym. Eng. Sci.* **1994**, *34*, 169–173.
- (20) Kapantaidakis, G. C.; Kaldis, S. P.; Dabou, X. S.; Sakellariopoulos, G. P. *J. Membr. Sci.* **1996**, *110*, 239–247.
- (21) Kapantaidakis, G. C.; Kaldis, S. P.; Sakellariopoulos, G. P.; Chira, E.; Loppinet, B.; Floudas, G. *J. Polym. Sci., Polym. Phys.* **1999**, *37*, 2788–2798.
- (22) Brekner, M.-J.; Schneider, H. A.; Cantow, H.-J. *Polymer* **1988**, *29*, 78–85.
- (23) Schneider, H. A. *Polymer* **1989**, *30*, 771–779.
- (24) Liang, K.; Grebowicz, J.; Valles, E.; Karasz, F. E.; MacKnight, W. J. *J. Polym. Sci., Polym. Phys.* **1992**, *30*, 465–476.
- (25) Koros, W. J.; Paul, D. R. *J. Polym. Sci., Polym. Phys. Ed.* **1976**, *14*, 675.
- (26) Maeda, Y.; Paul, D. R. *Polymer* **1985**, *26*, 2055–2063.
- (27) Morel, G.; Paul, D. R. *J. Membr. Sci.* **1982**, *10*, 273–282.

MA011672S